



Protein–protein interaction network and subcellular localization of the *Arabidopsis thaliana* ESCRT machinery

Lynn G. L. Richardson, Alexander S. M. Howard, Nicholas Khuu, Satinder K. Gidda, Andrew McCartney†, Brett J. Morphy and Robert T. Mullen*

Department of Molecular and Cellular Biology, University of Guelph, Guelph, ON, Canada

Edited by:

Chris Hawes, Oxford Brookes University, UK

Reviewed by:

Nadine Paris, Centre National de la Recherche Scientifique, France
Inhwan Hwang, Pohang University of Science and Technology, South Korea

*Correspondence:

Robert T. Mullen, Department of Molecular and Cellular Biology, University of Guelph, 488 Gordon Street, Guelph, ON, Canada.
e-mail: rtmullen@uoguelph.ca

†Present address:

Andrew McCartney, J.D. Irving Limited, Woodlands Division, Fredericton, NB, Canada.

The endosomal sorting complex required for transport (ESCRT) consists of several multi-protein subcomplexes which assemble sequentially at the endosomal surface and function in multivesicular body (MVB) biogenesis. While ESCRT has been relatively well characterized in yeasts and mammals, comparably little is known about ESCRT in plants. Here we explored the yeast two-hybrid protein interaction network and subcellular localization of the *Arabidopsis thaliana* ESCRT machinery. We show that the *Arabidopsis* ESCRT interactome possesses a number of protein–protein interactions that are either conserved in yeasts and mammals or distinct to plants. We show also that most of the *Arabidopsis* ESCRT proteins examined at least partially localize to MVBs in plant cells when ectopically expressed on their own or co-expressed with other interacting ESCRT proteins, and some also induce abnormal MVB phenotypes, consistent with their proposed functional role(s) as part of the ESCRT machinery in *Arabidopsis*. Overall, our results help define the plant ESCRT machinery by highlighting both conserved and unique features when compared to ESCRT in other evolutionarily diverse organisms, providing a foundation for further exploration of ESCRT in plants.

Keywords: *Arabidopsis*, endosome, ESCRT, interactome, multivesicular body, protein targeting, yeast two-hybrid

INTRODUCTION

In animal cells, plasma membrane proteins destined to be degraded are internalized via endocytosis and delivered through the endosomal pathway to the lysosome (Gruenberg and Stenmark, 2004). This sorting process is highly complex, involving the concentration of endocytosed membrane-bound, ubiquitinated cargo proteins within intraluminal vesicles of late endosomes or so-called multivesicular bodies (MVBs), which are derived from early (and recycling) endosomes by the progressive invagination and scission of their boundary membranes. Once formed, MVBs eventually fuse with the lysosome where their contents, including the intraluminal vesicles, are degraded.

The formation and scission of MVB intraluminal vesicles is unique, because, unlike other vesicle budding events (e.g., those mediated by clathrin or the coat protein complexes), it is directed away from the cytosol. This process is mediated by a set of ~30 soluble proteins collectively known as the endosomal sorting complex required for transport (ESCRT), which, in a sophisticated hierarchical- and stoichiometric-dependent manner, are assembled at the endosomal membrane into several multi-protein subcomplexes, termed ESCRT-0, -I, -II, and -III. First identified in the yeast *Saccharomyces cerevisiae* as class E vacuolar protein-sorting (Vps) proteins based on the observation that their mutations result in abnormal late endosomal structures termed class E compartments (Raymond et al., 1992), ESCRT proteins have been since found in a wide range of other evolutionarily diverse species, suggesting they perform a variety of conserved functions (Leung et al., 2008).

Current working models of the molecular mechanisms underlying ESCRT function have been the subject of several recent comprehensive reviews (Hurley and Hanson, 2010; Peel et al., 2010;

Roxrud et al., 2010), the details of which have come initially from yeast two-hybrid studies of the yeast and mammalian ESCRT interactomes followed by a proliferation in the past few years of biochemical, genetic, structural, and biophysical studies aimed at characterizing the role of ESCRT during MVB protein-sorting in these organisms. According to these models, ESCRT assembly begins with the recognition and concentration of ubiquitinated cargo proteins in the endosomal membrane by ESCRT-0 and the recruitment of ESCRT-I. ESCRT-I also binds and sorts ubiquitinated cargo, recruits ESCRT-II, and together, ESCRT-I and II induce membrane deformation. ESCRT-II additionally recruits ESCRT-III components, which oligomerize into higher-ordered polymers at the neck of the nascent vesicle that facilitate cargo protein sequestration and drive membrane scission resulting in the release of the nascent vesicle into the MVB lumen. Thereafter, ESCRT-III is disassembled and subsequently recycled back to the cytosol by the action of the AAA-type ATPase Vps4, a process that requires numerous protein regulators that ensure the proper recruitment and assembly of Vps4 and stimulate its activity. Interestingly, the ESCRT machinery, or at least portions thereof, also plays crucial roles in other important cellular processes, including enveloped retroviral budding, cytokinesis, and autophagy, all of which require membrane deformation and scission directed away from the cytosol (Carlton and Martin-Serrano, 2009).

In plants, the endosomal pathway is considered highly dynamic, but overall, is far less well understood compared to that of animals and yeasts. Nonetheless, several functional similarities exist, including roles in protein degradation, cytokinesis, receptor-mediated endocytosis, and intracellular signaling (Müller et al., 2007; Otegui and Spitzer, 2008; Robinson et al., 2008; Schellmann and Pimpl,

2009). The plant endosomal pathway is also involved in a number of key plant-specific processes, including embryo differentiation and the regulation of auxin transport (Otegui and Spitzer, 2008). Plants, like yeasts and animals, also possess MVBs (also referred to as prevacuolar compartments; Mo et al., 2006) that act as protein-sorting junctions for processes including ESCRT-mediated trafficking of ubiquitinated membrane proteins to the vacuole for degradation. However, the biogenetic relationship between MVBs and other compartments of the endosomal pathway in plant cells is not entirely clear. Plants, for instance, do not appear to possess early endosomes like those that mature into MVBs in mammals. Moreover, multiple types of MVBs as well as vacuoles appear to exist in plant cells, all of which may have different functions depending on the tissue or organ that they reside in and/or the developmental stage (Otegui and Spitzer, 2008).

As listed in **Table 1**, homologs of all of the main ESCRT and ESCRT-associated proteins in yeasts and mammals, with the exception of those comprising ESCRT-0 (i.e., Vps27/HRS, HseI/STAM) and the ESCRT-I component Mvb12, exist in *Arabidopsis thaliana* (Mullen et al., 2006; Spitzer et al., 2006; Winter and Hauser, 2006; Leung et al., 2008). However, only a few of these proteins and/or their homologs in other plant species have been analyzed experimentally, and to varying degrees (Shen et al., 2003; Yang et al., 2004; Jou et al., 2006; Haas et al., 2007; Tian et al., 2007; Spitzer et al., 2009; Shahriari et al., 2010). While each of these studies has provided important functional insights to the plant ESCRT machinery, experimental data for the overall organization of ESCRT in plants compared to other organisms are lacking, and virtually non-existent for the putative components of ESCRT-II and ESCRT-III. Furthermore, like other non-opisthokonts (e.g., *Dictyostelium*, *Chlamydomonas*), plants lack an ESCRT-0 complex, but they possess a family of proteins homologous to the target of myb 1 (Tom1) proteins that in mammals, participate in ubiquitinated cargo sorting, bind ESCRT-I, and are thought to function in parallel with ESCRT-0 (Wang et al., 2010). Thus, plant Tom1 proteins have been also proposed, but not tested experimentally, to function as a so-called “alternate” ESCRT-0 complex during MVB biogenesis (Winter and Hauser, 2006; Leung et al., 2008).

Here we begin to address the paucity in our understanding of the plant ESCRT machinery by examining many of the known and putative components of *Arabidopsis* ESCRT in terms of their protein–protein interaction network using yeast two-hybrid assays and subcellular localization(s) in transiently transformed suspension-cultured tobacco cells. We discuss the results of these studies primarily in terms of the current working models of ESCRT’s role during MVB biogenesis in yeast and mammalian model systems and, in doing so, we highlight not only evolutionarily conserved aspects of the plant ESCRT machinery, but also unique features which may reflect the functional plasticity of ESCRT in plants.

MATERIALS AND METHODS

RECOMBINANT DNA PROCEDURES AND PLASMID CONSTRUCTION

Molecular biology reagents were purchased either from New England BioLabs, Promega, Perkin Elmer Life Sciences Inc., Stratagene, or Invitrogen. Oligonucleotides were synthesized by Sigma-Aldrich or University of Guelph Laboratory Services. DNA was isolated and purified using reagents from Invitrogen. All DNA constructs were

verified using dye-terminated cycle sequencing performed at the University of Guelph Genomics Facility. Mutagenesis was carried out using appropriate complementary forward and reverse mutagenic primers and the QuikChange site-directed mutagenesis kit according to the manufacturer’s instructions (Stratagene).

cDNAs encoding full-length open reading frames (ORF) for various *Arabidopsis* ESCRT components were obtained from the *Arabidopsis* Biological Resource Center (Ohio State University) or RIKEN Bioresource Center and then, using PCR and the appropriate forward and reverse primers, were sub-cloned into one or more of the following plasmids: the yeast (two-hybrid) expression vectors pGADT7 and pGBKT7 (Clontech; distributed by BD Bioscience), consisting of sequences encoding (in pGADT7) the GAL4 activation domain (AD) and an hemagglutinin (HA)-epitope tag followed by a multiple cloning site (MCS), or (in pGBKT7) the GAL4 DNA-binding domain (BD) and a Myc-epitope tag, followed by an MCS; pRLT2/Myc-MCS, a plant expression vector that includes the 35S cauliflower mosaic virus (CMV) promoter and sequences encoding an initiation methionine and Myc-epitope tag, then an MCS (Shockey et al., 2006); pRTL2/HA-MCS, which is equivalent to pRTL2/Myc-MCS, except that it contains sequences encoding an HA epitope tag; pRTL2/GFP-MCS and pUC18/*NheI*-GFP, both of which contain the 35S CMV promoter, but differ in that an MCS or unique *NheI* restriction site is either immediately 3’ or 5’ of the green fluorescent protein (GFP) ORF, respectively (Shockey et al., 2006; Clark et al., 2009). Complete details on the construction procedures used for generating plasmids encoding any of the various *Arabidopsis* ESCRT components (or modified versions thereof) used in this study are available upon request.

pUC18/GFP-Syp21 encodes GFP fused to the N terminus of the *Arabidopsis* membrane-bound Qa-SNARE (soluble *N*-ethylmaleimide-sensitive factor attachment protein receptor) Syp21 (Syntaxin of plants 21; Ueda et al., 2001) and pBSIIKS+/GFP-ARA7 encodes the *Arabidopsis* Rab5 (Rabenosyn-5)-related GTPase Ara7 fused to the C terminus of GFP (Uemura et al., 2004). pBSIIKS+/GFP-ARA7 was used for the construction of pRTL2/RFP-Ara7, whereby the Ara7 ORF was sub-cloned (via PCR) into pRTL2/RFP-MCS, containing the red fluorescent protein (RFP) ORF followed by an MCS (Shockey et al., 2006). pCam-YFP-Rab5/F2a encodes the yellow fluorescent protein (YFP) fused to the N terminus of the *Arabidopsis* Rab5-related GTPase Rha1 (also referred to as RabF2a; Haas et al., 2007) and pMO4-AtSKD1[E232Q] encodes GFP fused to the N terminus of a mutant version of *Arabidopsis* SKD1 (referred to hereafter as Vps4), whereby the glutamic acid residue at position 232 of Vps4 was replaced with a glutamine (Vps4^{E232Q}), resulting in an ATP hydrolysis deficiency (Haas et al., 2007).

YEAST TWO-HYBRID AND β -GALACTOSIDASE ASSAYS

The Clontech Matchmaker GAL4 Two-Hybrid System 3 (BD Bioscience) was used according to the manufacturer’s instructions, with some modifications. Briefly, yeast cells (strain PJ69-4A) harboring pGADT7 (bait) and/or pGBKT7 (prey) plasmids were cultured in duplicate in synthetic dextrose medium [2% (w/v) dextrose, 0.67% (w/v) yeast nitrogen base without amino acids, 2 g L⁻¹ synthetic mix of amino acid supplements, minus leucine, and tryptophan; SD-LT; Bufferad] and plated [at equal cell density

Table 1 | Endosomal sorting complex required for transport and ESCRT-associated proteins in yeasts, mammals, and *Arabidopsis*.

Complex	Yeast ^a	Mammals ^a	<i>Arabidopsis</i> ^b		Complex	Yeast ^a	Mammals ^a	<i>Arabidopsis</i> ^b		
			Protein ^c	AGI ^d				Protein ^c	AGI ^d	
ESCRT-0 Other proteins known or proposed to be involved in ubiquitinated cargo protein-sorting and/or interaction with ESCRT-I	Vps27	HRS				Vps20	CHMP6	Vps20A	At5g09260	
	Hse1	STAM1						Vps20B	At5g63880	
		STAM2				Vps24	CHMP3	Vps24A	At5g22950	
		Tom1L1	Tom1A	At2g38410				Vps24B	At3g45000	
						Snf7/Vps32	CHMP4A	Snf7A	At2g19830	
								(Vps32.1)		
							CHMP4B	Snf7B	At4g29160	
								(Vps32.2)		
							CHMP4C			
						Vps4 and associated regulators	Vps4	VPS4A	Vps4	At2g27600
								(SKD1)		
								VPS4B		
	ESCRT-II	Vps23	VPS23/ TSG101	Vps23A (ELC)	At3g12400		Vps60	CHMP5	Vps60A	At3g10640
			Vps23B (ELC-like)	At5g13860				Vps60B	At5g04850	
Vps28		VPS28	Vps28A	At4g05000		Did2/Vps46	CHMP1A	Chmp1A	At1g73030	
			Vps28B	At4g21560				Chmp1B	At1g17730	
Vps37		VPS37A	Vps37A	At3g53120		Bro1/Vps31	ALIX/AIP1	Bro1	At1g15130	
		VPS37B	Vps37B	At2g36680		Vta1	VTA1/LIP5	Vta1	At4g26750	
		VPS37C						(LIP5)		
		VPS37D								
		Mvb12	MVB12							
		Vps22	EAP30	Vps22	At4g27040					
		Vps25	EAP20	Vps25	At4g19003					
		Vps36	EAP45	Vps36	At5g04920					
ESCRT-III		Vps2/Did4	CHMP2A	Chmp2A	At2g06530					
		CHMP2B	Chmp2B	At5g44560						
			Chmp2C	At1g03950						

^aNomenclature of yeast (*S. cerevisiae*) and mammalian (human) ESCRT and ESCRT-associated proteins is based on those previously published (Hurley and Hanson, 2010), including for the *Arabidopsis* Tom1 proteins (Winter and Hauser, 2006). ^b*Arabidopsis* ESCRT and ESCRT-associated proteins were identified previously using BLASTp analyses with amino acid sequences of known class E Vps proteins from yeasts and humans as queries (Mullen et al., 2006; Spitzer et al., 2006; Winter and Hauser, 2006), or using comparative genomic analyses of coding sequences (Leung et al., 2008). ^cNomenclature of *Arabidopsis* ESCRT and ESCRT-associated proteins used in this study. Alternate nomenclature of selected *Arabidopsis* proteins indicated in brackets are based on Spitzer et al. (2006), Haas et al. (2007) and Shahriari et al. (2010). ^d*Arabidopsis* gene identifier (AGI) number represents the systematic designation given to each locus, gene, and its corresponding protein product(s) by the *Arabidopsis* Information Resource (<http://www.arabidopsis.org>). Alix, ALG-2-interacting protein x; Aip1, apoptosis-linked gene (ALG)-2-interacting protein; Bro1, bypass requirement for protein kinase C homolog (BCK) 1-like resistance to osmotic shock; Chmp, charged multivesicular body protein; Did2, DOA4-independent degradation 2; EAP, RNA polymerase II elongation factor ELL-associated protein; ELC, elch (German for elk); HRS, hepatocyte growth factor-regulated tyrosine kinase substrate; LIP5, lysosomal trafficking regulator (lyst) interacting protein 5; Snf7, sucrose non-fermenting 7; STAM, signal-transducing adaptor molecule; TSG101, tumor susceptibility gene 101; SKD1, suppressor of K⁺ transport growth defect 1; Hsel, Hbp, STAM, and EAST; Tom1, target of myb 1; Vta1, Vps20-associated 1.

(0.1 OD₆₀₀) on either SD-LT (low-stringency selection media), SD-LTHA (SD-LT medium that also lacked histidine and adenine; high-stringency selection media), or SD-LTHA plus 15 mM 3-amino-1,2,4-triazole (3-AT), which is used to inhibit low levels of His3 activity, and thus, suppress background growth due to “auto-activation” of the *HIS3* reporter gene. The relative growth rates of cells (compared to each other and to cells containing positive or negative control “bait” and “prey” plasmid pairs provided by Clontech) were assessed daily (up to 5 days) as either: no growth or

weak, medium, or strong growth. Results of growth assays are based on three separate experiments performed using all of the respective genes (other than those that “autoactivated” in the presence of 3-AT) both as “bait” and “prey.” Activation of the lacZ reporter and determination of the resulting β-galactosidase (β-Gal) activity in co-transformed yeast strains cultured in SD-LT was carried out using a Semi-quantitative β-Gal Assay kit (Pierce Protein Research Products) and a Molecular Devices Thermo Max microplate reader to detect β-gal product (o-nitrophenol) formation at OD₆₀₀. β-Gal

enzyme activity was calculated in Miller units (Miller, 1972) and based on the average activity of at least three replicates from three separate (yeast) co-transformations.

YEAST PROTEIN EXTRACTS AND WESTERN BLOT ANALYSIS

Protein lysates of yeast strains transformed individually with *Arabidopsis* ESCRT plasmids were prepared as described by O'Quin et al. (2009). Proteins were separated on 10% SDS-PAGE gels and stained with Coomassie blue R250 to verify approximately equal loading of total protein or, for Western blotting, proteins were transferred to nitrocellulose membranes using a semi-dry transfer cell (Bio-Rad Laboratories). Membranes were probed with either rabbit α -Myc, rabbit α -HA (Bethyl Laboratories), or mouse α -HA (Covance) primary antibodies and goat α -rabbit or rabbit α -mouse secondary antibodies conjugated to peroxidase (Sigma). Proteins were immunodetected using the Western Lightning[®] Chemiluminescence Reagent Plus kit (Perkin Elmer) and membranes were exposed to Kodak X-OMAT Blue XB film and developed using a Konica Minolta SRX-101A film processor.

IN VITRO CO-IMMUNOPRECIPITATIONS

Hemagglutinin- or Myc-tagged proteins were synthesized *in vitro* using the TNT T7 Coupled Reticulocyte Lysate System (Promega) according to the manufacturer's protocol, with the corresponding pGADT7 or pGBKT7 *Arabidopsis* ESCRT plasmids serving as template DNA. *In vitro* co-immunoprecipitations were carried out essentially as described in the Clontech Matchmaker Co-IP kit user manual. Specifically, immunoprecipitation of "bait" proteins were carried out using either rabbit α -HA or mouse α -Myc antibodies in hybridoma medium (clone 9E10; Princeton University Monoclonal Antibody Facility) and protein A-Sepharose beads (Sigma-Aldrich). SDS-PAGE and Western blotting of co-immunoprecipitated proteins were performed as described above.

BIOLISTIC BOMBARDMENT AND FLUORESCENCE MICROSCOPY

Tobacco [*Nicotiana tabacum* cv Bright-Yellow-2 (BY-2)] suspension cell cultures were maintained and prepared for biolistic bombardment as described previously (Lingard et al., 2008). Transient (co-)transformations were performed using 0.5–6 μ g of plasmid DNA [determined empirically based on the relative strength of the (immuno)fluorescence signal due to expression levels of each plasmid-encoded protein construct] with a biolistic particle delivery system-1000/HE (Bio-Rad Laboratories). Bombarded cells were incubated for ~4–8 h to allow for expression and sorting of the introduced gene product(s) and to reduce potential negative effects due to protein over-expression. Cells were either viewed immediately or fixed in 4% (w/v) formaldehyde, followed by permeabilization with 0.01% (w/v) pectolyase Y-23 (Kyowa Chemical Products) and 0.3% (v/v) Triton X-100 (Sigma-Aldrich). Antibodies used for subsequent immunofluorescence staining of cells were as follows: mouse α -Myc antibodies; rabbit α -Myc; rabbit α -HA; goat α -mouse and goat α -rabbit Alexa Fluor 488 IgGs, goat α -mouse and goat α -rabbit Cy5 (Cedar Lane Laboratories); and goat α -rabbit rhodamine red-X IgGs (Jackson ImmunoResearch Laboratories).

Epifluorescent images of cells were acquired using an AxioScope 2 MOT epifluorescence microscope (Carl Zeiss Inc.) with a 63 \times Plan Apochromat oil-immersion objective. Image capture was

performed using a Retiga 1300 CCD camera (Qimaging) and Openlab software (Improvision). Confocal laser-scanning microscopy (CLSM) was carried out using a Leica DM RBE microscope with a 63 \times Plan Apochromat oil-immersion objective, anTCS SP2 scanning head, and the TCS NT software. Fluorophore emissions were collected sequentially in double- and triple-labeling experiments; single-labeling experiments showed no detectable crossover at the settings used for data collection. Other negative controls including omission of primary or secondary antibodies and mock transformations with vector (pRTL2) alone also yielded no detectable fluorescence. Confocal images were acquired as a z-series or single optical sections of representative cells were saved as 512 \times 512-pixel digital images. Figure compositions and merged images were generated using Northern Eclipse software (Empix Imaging Inc.) and Adobe Photoshop CS or Illustrator CS2 (Adobe Systems). The co-localization of proteins in selected CLSM optical sections was quantified using the ImageJ plugin "Co-localization Finder" and methods based on those described previously by us (Gidda et al., 2011).

In all experiments, at least 50 independently (co-)transformed cells were evaluated to determine subcellular localization(s) of transiently (co)expressed proteins, and all micrographs shown in the figures are representative images. Each biolistic experiment was replicated at least two times.

RESULTS AND DISCUSSION

ARABIDOPSIS ESCRT PROTEIN INTERACTOME

As mentioned in the Introduction, considerable effort has been devoted previously to generating yeast two-hybrid-based protein–protein interactomes for the ESCRT machinery in both yeasts and mammals (Nikko and André, 2007 and references therein). All of these studies took advantage of the robust and high-throughput nature of the yeast two-hybrid assay to identify the multitude of protein–protein interactions that occur within and between the ESCRT subcomplexes in these organisms, providing the foundation for most of the subsequent biochemical, genetic, and structural studies of ESCRT, leading to current working models of ESCRT assembly and function.

Here we also employed the yeast two-hybrid system to characterize the *Arabidopsis* ESCRT interactome. DNA sequences encoding most of the known or putative *Arabidopsis* ESCRT proteins listed in **Table 1** were cloned as both GAL4-AD and GAL4-DNA-BD fusions, allowing for the detection of self-interactions and those interactions that may have been otherwise absent due to interference from either the AD or BD fusion tag. Each of the AD/BD-ESCRT fusions were also introduced individually into yeast to confirm that they were properly expressed (**Figure S1** in Supplementary Material) and that they did not "autoactivate" the two-hybrid reporter gene system on their own. Interactions among *Arabidopsis* ESCRT proteins were then assessed in two ways. First, the relative growth rates of co-transformed yeast were compared on selection media with or without 3-AT, and all positive interactions were then scored based on growth as either weak, medium, or strong; refer to **Figure S2** in Supplementary Material for an example of the relative growth of yeast expressing positive-interacting ESCRT proteins. Second, all positive interactions detected by growth assays were quantified using liquid β -Gal assays. We also verified at least some of

the results of our yeast two-hybrid assays by carrying out co-immunoprecipitations with selected *in vitro*-synthesized Myc- or HA-epitope-tagged ESCRT proteins (Figure S3 in Supplementary Material). However, the low efficiency of *in vitro* translation for many of the ESCRT proteins precluded us from validating a large number of interactions using this method. Nonetheless, the results from our yeast two-hybrid assays, as discussed below, revealed not only several new interactions for *Arabidopsis* ESCRT proteins, but also reconfirmed almost all of the interactions previously published for selected *Arabidopsis* ESCRT proteins using the same (yeast two-hybrid) or other [e.g., immunoprecipitations or biomolecular fluorescence complementation (BiFC)] interaction methods, hence validating the reliability of this assay for mapping the *Arabidopsis* ESCRT interactome overall.

As summarized in the matrix presented in Figure 1, the overall pattern of the *Arabidopsis* ESCRT protein interactome reflects well the conservation of the hierarchical manner in which the ESCRT machinery is assembled during MVB biogenesis across evolutionarily diverse species. That is, analogous to the interactions reported

for mammalian and/or yeast ESCRT proteins during the assembly process, the majority of interactions detected between *Arabidopsis* ESCRT proteins were those within and between multi-protein subcomplexes that function sequentially in MVB biogenesis, suggesting that these interactions are mechanistically equivalent in plants. For example, the ESCRT-I components Vps23A and Vps23B, displayed numerous interactions that likely reflect their conserved importance in ESCRT-I assembly (e.g., Vps23A/B-Vps23A/B, Vps23A/B-Vps37A and Vps23A/B-Vps28A/B) and in the recruitment of ESCRT-II (e.g., Vps23A/B-Vps25, Vps23A/B-Vps22, and Vps23A/B-Vps36; Figure 1) in *Arabidopsis*. However, unlike mammals and yeast, plants appear to be devoid of a fourth ESCRT-I component, Mvb12, which regulates the cargo protein-sorting activity of ESCRT-I (Leung et al., 2008). Thus, plants might rely on a separate mechanism for this process.

We also observed interactions between various *Arabidopsis* ESCRT-I components and members of the Tom1 family of proteins. Specifically, Vps23A/B, Vps28A/B, and Vps37A all interacted with Tom1D, and Vps23B interacted also with Tom1A/F/L/G (Figure 1).

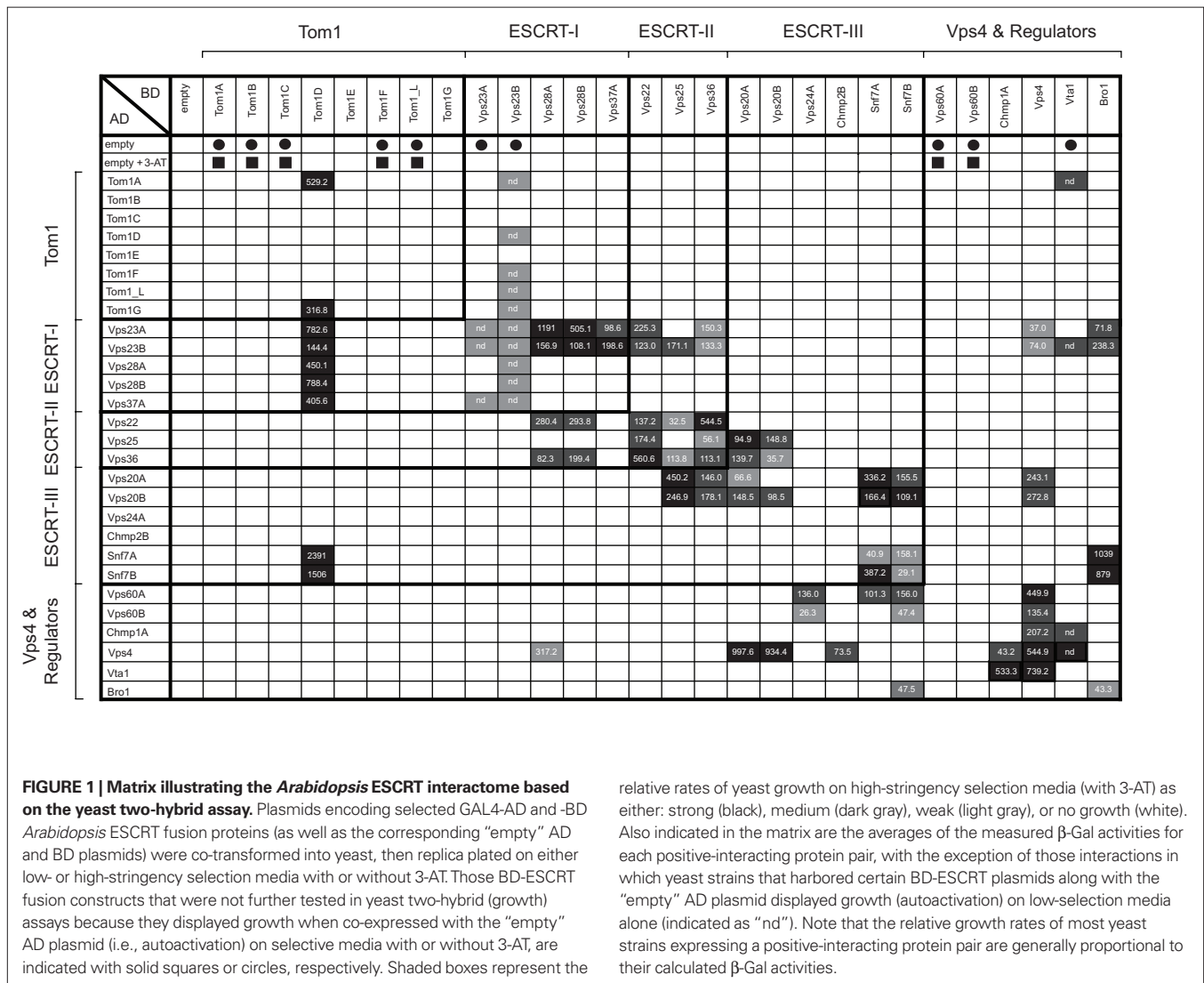


FIGURE 1 | Matrix illustrating the *Arabidopsis* ESCRT interactome based on the yeast two-hybrid assay. Plasmids encoding selected GAL4-AD and -BD *Arabidopsis* ESCRT fusion proteins (as well as the corresponding “empty” AD and BD plasmids) were co-transformed into yeast, then replica plated on either low- or high-stringency selection media with or without 3-AT. Those BD-ESCRT fusion constructs that were not further tested in yeast two-hybrid (growth) assays because they displayed growth when co-expressed with the “empty” AD plasmid (i.e., autoactivation) on selective media with or without 3-AT, are indicated with solid squares or circles, respectively. Shaded boxes represent the

relative rates of yeast growth on high-stringency selection media (with 3-AT) as either: strong (black), medium (dark gray), weak (light gray), or no growth (white). Also indicated in the matrix are the averages of the measured β -Gal activities for each positive-interacting protein pair, with the exception of those interactions in which yeast strains that harbored certain BD-ESCRT plasmids along with the “empty” AD plasmid displayed growth (autoactivation) on low-selection media alone (indicated as “nd”). Note that the relative growth rates of most yeast strains expressing a positive-interacting protein pair are generally proportional to their calculated β -Gal activities.

Moreover, co-immunoprecipitation assays confirmed the binding between Vps23A/B and Tom1D as well as the apparent lack of binding between Vps23A/B and Tom1A or Tom1C (**Figure S3** in Supplementary Material). These data are consistent with the proposal that specific Tom1 proteins may act as an alternate ESCRT-0 complex in plants (Winter and Hauser, 2006; Leung et al., 2008), as may be also the case in *Dictyostelium*, which lacks an ESCRT-0 complex, but possesses a Tom1 homolog that binds Tsg101 (Blanc et al., 2009). Of course the lack of interaction between other Tom1 proteins and Vps23A/B in this study (**Figure 1**) does not preclude an interaction in plant cells, given the general limitations of the yeast two-hybrid assay, such as BD-fusion-protein “autoactivation” (e.g., Tom1A/B/C/F/_L) or the absence of additional endogenous interacting proteins and/or membranes. Thus, subsequent examination of these and other *Arabidopsis* ESCRT proteins in terms of validating these interactions (or lack thereof) using complementary experimental approaches is still required. Further work is needed to also confirm and clarify the functional implications of Tom1 proteins as a possible alternate ESCRT-0 complex in *Arabidopsis*, including whether they bind to and mediate cargo protein-sorting.

In addition to interacting with components of ESCRT-I, we showed that the putative *Arabidopsis* ESCRT-II components, Vps22 and Vps36, interacted with themselves and each other, as well as with the other (third) putative component of ESCRT-II, Vps25 (**Figure 1**). Moreover, the binding of Vps36 and Vps25 was confirmed by co-immunoprecipitation (**Figure S3** in Supplementary Material). Vps25 and Vps36 also interacted with the putative ESCRT-III components Vps20A/B and Snf7A/B (**Figure 1**; **Figure S3** in Supplementary Material). These interactions have not been previously shown for plants and are consistent with yeast and mammalian models for ESCRT-II assembly and the role of ESCRT-II in the recruitment and assembly of ESCRT-III (Hurley and Hanson, 2010; Peel et al., 2010). That is, ESCRT-II is thought to be recruited to the endosomal surface via an interaction between ESCRT-I and Vps36/Eap45, and is assembled into a core complex composed of one copy each of Vps22/Eap30 and Vps36/Eap45, both of which are bound to a molecule each of Vps25/Eap20. Thereafter, Vps25/Eap20 interacts with Vps20/Chmp6 of ESCRT-III, which subsequently binds to Snf7/Chmp4 and serves as an active nucleator for Snf7/Chmp4 oligomerization, leading to the final assembly steps of the ESCRT-III polymer complex, membrane scission and formation of an internal vesicle within the MVB. Notably, the putative *Arabidopsis* Snf7A and Snf7B proteins are also capable of homotypic and heterotypic interactions (**Figure 1**), consistent with a conserved role for Snf7 oligomerization during ESCRT-III assembly in plants.

On the other hand, we found that Snf7A/B and Vps20A/B, did not interact with the other two putative components of the *Arabidopsis* ESCRT-III complex, i.e., Vps24A and Chmp2B (**Figure 1**). These results were somewhat unexpected given the reported binding behaviors and proposed roles of their counterparts in other organisms. For example, in yeast, Vps24 and Vps2 (the homolog of mammalian and *Arabidopsis* Chmp2) interact to form a subcomplex that then binds to the Vps20-Snf7 subcomplex, yielding the core ESCRT-III complex (Hurley and Hanson, 2010; Peel et al., 2010). While the apparent lack of interaction between *Arabidopsis* Vps24A and Chmp2B with other ESCRT-III components may reflect, as men-

tioned above, a general limitation of the yeast two-hybrid assay, it is also possible that it represents plant-specific differences in ESCRT-III assembly. Hence, both possibilities require further investigation.

Following membrane scission, the disassembly of ESCRT-III in yeasts and mammals is mediated by the recruitment of the AAA-ATPase Vps4 and several of its regulatory factors, including Ist1 and Did2/Chmp1, to the endosomal membrane. Additional Vps4 regulatory factors are then also recruited, including Vps60 and Vta1/LIP5, both of which induce the assembly of Vps4 into an active oligomer and stimulate ATP hydrolysis (reviewed in Hurley and Hanson, 2010; Peel et al., 2010). While no interactions were observed in this study between any of the putative *Arabidopsis* ESCRT-III proteins and the Vps4 regulators Chmp1A or Vta1, between Vta1 and the other putative Vps4 regulators, Vps60A/B, or, in contrast to the results recently reported by Shahriari et al. (2010), between Vps4 and Snf7A/B, we did observe interactions between Vps24A and Vps60A/B, as well as between Chmp2B and Vps4 (**Figure 1**). Moreover, as reported previously using *in vitro* co-immunoprecipitations (Haas et al., 2007; Spitzer et al., 2009) or yeast two-hybrid and/or BiFC assays (Shahriari et al., 2010), we observed interactions between Chmp1A and Vta1 with Vps4 (**Figure 1**; **Figure S3** in Supplementary Material). We also found that Vps4 interacted with Vps20A/B and Vps60A/B, similar to their reported interactions via BiFC (Shahriari et al., 2010), and Vps4 also displayed homotypic binding (**Figure 1**), just as it does in other (non-plant) organisms (Shestakova et al., 2010).

Taken together, the interaction results for components of *Arabidopsis* ESCRT-III, Vps4, as well as the various Vps4 regulators, further support our conclusion that while generally conserved with respect to the interactions that take place between their counterparts in yeasts and/or mammals, the *Arabidopsis* ESCRT machinery also possesses a number of unique differences that may reflect the functional plasticity of the plant ESCRT system overall. Indeed, given the number of different isoforms for several of the subunits of the *Arabidopsis* ESCRT-III complex, as well as the Vps4 regulators (**Table 1**), and that, compared to yeasts and mammals, the endosomal system in plants appears to be more complex in terms of its organization and trafficking pathways (Otegui and Spitzer, 2008; Robinson et al., 2008), it is not altogether surprising that these proteins, and perhaps other uncharacterized proteins interact and operate in additional and/or different ways in plants.

SUBCELLULAR LOCALIZATION OF *ARABIDOPSIS* ESCRT PROTEINS

We next characterized the *Arabidopsis* ESCRT machinery by examining the subcellular localization of some of the known and putative ESCRT proteins in tobacco BY-2 suspension-cultured cells, which serve as a well-known model plant cell system for studying protein targeting and organelle biogenesis (Brandizzi et al., 2003; Miao and Jiang, 2007). Specifically, epitope- or fluorescent protein-tagged versions of selected ESCRT proteins from **Table 1**, including one or more proteins from each of the various ESCRT subcomplexes, as well as Vps4, or modified versions thereof, were expressed transiently (via biolistic bombardment) either individually or in combination in BY-2 cells. Their resulting subcellular localizations were then assessed, along with that of the co-expressed MVB marker protein, GFP-Syp21, consisting of GFP appended to the N terminus of the *Arabidopsis* membrane-bound Qa-SNARE Syp21 (Uemura

et al., 2004), by standard epifluorescence microscopy, and/or by CLSM, when greater spatial resolution was necessary in order to confirm protein co-localization on a single optical plane or to view a novel MVB-related structure(s) in a 3D distribution. We also chose to examine the subcellular localization of selected plant ESCRT proteins in order to complement the protein–protein interaction results from our yeast two-hybrid assays (Figure 1), as well as the wealth of information already available on the ESCRT-related functions and/or MVB targeting mechanisms of their homologs in yeasts and mammals. In doing so, this allowed us to discuss these (*Arabidopsis*) proteins in terms of the current, generalized working models for ESCRT.

As shown in Figure 2A, N-terminal Myc-epitope-tagged versions of various members of the *Arabidopsis* Tom1 protein family displayed either (for Tom1A and Tom1D) a diffuse cytosolic and small punctate fluorescence pattern or (for Tom1C and Tom1E) an exclusively cytosolic fluorescence pattern, all of which were distinct from the punctate/globular fluorescence pattern attributable to GFP-Syp21 in the same representative co-transformed BY-2 cells, suggesting that these Tom1 proteins do not localize at steady state to MVBs. Moreover, the punctate structures observed in Myc-Tom1D-expressing cells did not colocalize with other endosomal pathway marker proteins, including those for the *trans*-Golgi or vacuole (data not shown). We also found that the subcellular localization of each of the selected Tom1 proteins was not affected by their co-expression with GFP-Syp21, since similar localization results were observed when Myc-Tom1A/C/D/E were expressed on their own (Figure 2B). Moreover, Tom1A-Myc (consisting of the Myc-epitope appended to the C terminus of Tom1A) and GFP-Tom1A (consisting of GFP appended to the N terminus of Tom1A), similar to Myc-Tom1A, localized to both the cytosol and small punctae in formaldehyde-fixed or living BY-2 cells, which were co-transformed with GFP-Syp21 or RFP-Ara7, respectively (Figures 2C,D); RFP-Ara7 serving as another well characterized endosomal (MVB) marker fusion protein consisting of RFP fused to the N terminus of the *Arabidopsis* Rab5-related soluble GTPase, Ara7 (Lee et al., 2004; Ueda et al., 2004). Collectively, these results indicate that the subcellular localization of the Tom1 proteins is not influenced by their appended epitope or fluorescent protein tags, or despite modest changes in endosome morphology due to formaldehyde fixation.

While the appearance (i.e., number, size, and distribution) of GFP-Syp21- or RFP-Ara7-labeled MVBs in BY-2 cells co-expressing selected Tom1 proteins (or other ESCRT or ESCRT-associated proteins) often varied among cells, this variability has been also reported for other plant cell types and was expected given the highly dynamic nature of the plant endosomal system overall. In addition, over-expression of Syp21 has been previously shown to prevent fusion of MVBs with the vacuole, leading to accumulation of vacuole-destined proteins at MVBs, ultimately resulting in the formation of enlarged MVBs (Foresti et al., 2006). Regardless, in a series of control experiments (Figure 2E), we confirmed that GFP-Syp21 partially colocalized with co-expressed RFP-Ara7, while YFP-Rha1, consisting of YFP fused to Rha1, another MVB-localized *Arabidopsis* Rab5-related GTPase (Lee et al., 2004), partially colocalized with co-expressed RFP-Ara7, and that in both sets of co-transformed cells at least some of the MVBs appeared

to be enlarged and/or aggregated (i.e., clustered in certain regions of these cells); the partial co-localization between GFP-Syp21 and RFP-Ara7 also verified by CLSM (Figure 2F) and quantified based on the mean Pearson's correlation coefficient r , which revealed a significant amount of fluorescence signal overlap ($r = 0.67 \pm 0.09$; see Materials and Methods for details). Overall, these results match those from similar experiments which showed that Ara7/Rha1 and Syp21 are preferentially localized in at least two types of partially overlapping and structurally related endosomal (MVB) compartments in plant cells (Lee et al., 2004; Ueda et al., 2004; Foresti et al., 2010). For the remainder of experiments described in this study, however, we chose to utilize GFP-Syp21 as a marker for MVBs, since, for among other reasons, it represents one of the best characterized MVB marker proteins in terms of its trafficking and biological activities (Shirakawa et al., 2010; Uemura et al., 2010). We also attempted to control for any potential negative effects due to GFP-Syp21 over-expression (Foresti et al., 2006), or transient protein (over)expression in general, by focusing on cells exhibiting relatively low or moderate levels of (immuno)fluorescence, as previously described (e.g., Ueda et al., 2004; Kato et al., 2010). In addition, as we did for with the abovementioned Tom1 proteins, all of the other ESCRT or ESCRT-associated proteins examined in this study in terms of their localization in BY-2 cells were expressed on their own to assess the effects of co-expression with GFP-Syp21 and/or other ESCRT proteins.

Given that both *Dictyostelium* Tom1 and human Tom1L1 bind Tsg101 (Yanagida-Ishizaki et al., 2008; Blanc et al., 2009) we tested further whether the *Arabidopsis* Tom1 proteins, using Tom1A and Tom1D as representatives of this group [i.e., both proteins bound Vps23A and/or Vps23B in yeast two-hybrid assays (Figure 1)], are redistributed to MVBs when co-expressed with Vps23A, which represents the best characterized component of ESCRT-I in plants (Spitzer et al., 2006). As shown in Figure 3, HA-Vps23A partially colocalized with co-expressed GFP-Syp21 in MVBs in BY-2 cells ($r = 0.62 \pm 0.13$), as expected (Spitzer et al., 2006). Figure 3 shows also that Myc-Tom1A partially localized to HA-Vps23A-containing structures ($r = 0.59 \pm 0.12$) that, based on the co-localization of HA-Vps23A and GFP-Syp21, were presumed to be MVBs. By contrast, Myc-Tom1D co-expressed with HA-Vps23A was not redirected to HA-Vps23A-containing MVBs ($r = 0.22 \pm 0.07$), but rather remained localized in the cytosol and small punctae in these cells (Figure 3), similar to when it is either expressed on its own or co-expressed with GFP-Syp21 (Figure 2). Additionally, we showed that GFP-Tom1A partially colocalized with Myc-Vps23B in co-transformed cells (Figure 3; $r = 0.61 \pm 0.06$), suggesting that Vps23A and Vps23B are equivalent in terms of their ability to recruit Tom1A to MVBs.

That Tom1D, unlike Tom1A, is not recruited to MVBs upon co-expression of Vps23A/B was unexpected, given their high degree of sequence similarity and comparable domain organization (Winter and Hauser, 2006), as well as their shared ability to interact with ESCRT-I components in yeast two-hybrid assays (Figure 1). We speculate that this may be due to stoichiometric differences in the relative amounts of these co-expressed proteins and/or additional endogenous factors. Regardless, the co-localization of Tom1A and Vps23 observed in this study is consistent with the localization of Tom1-related proteins in other organisms (Yanagida-Ishizaki

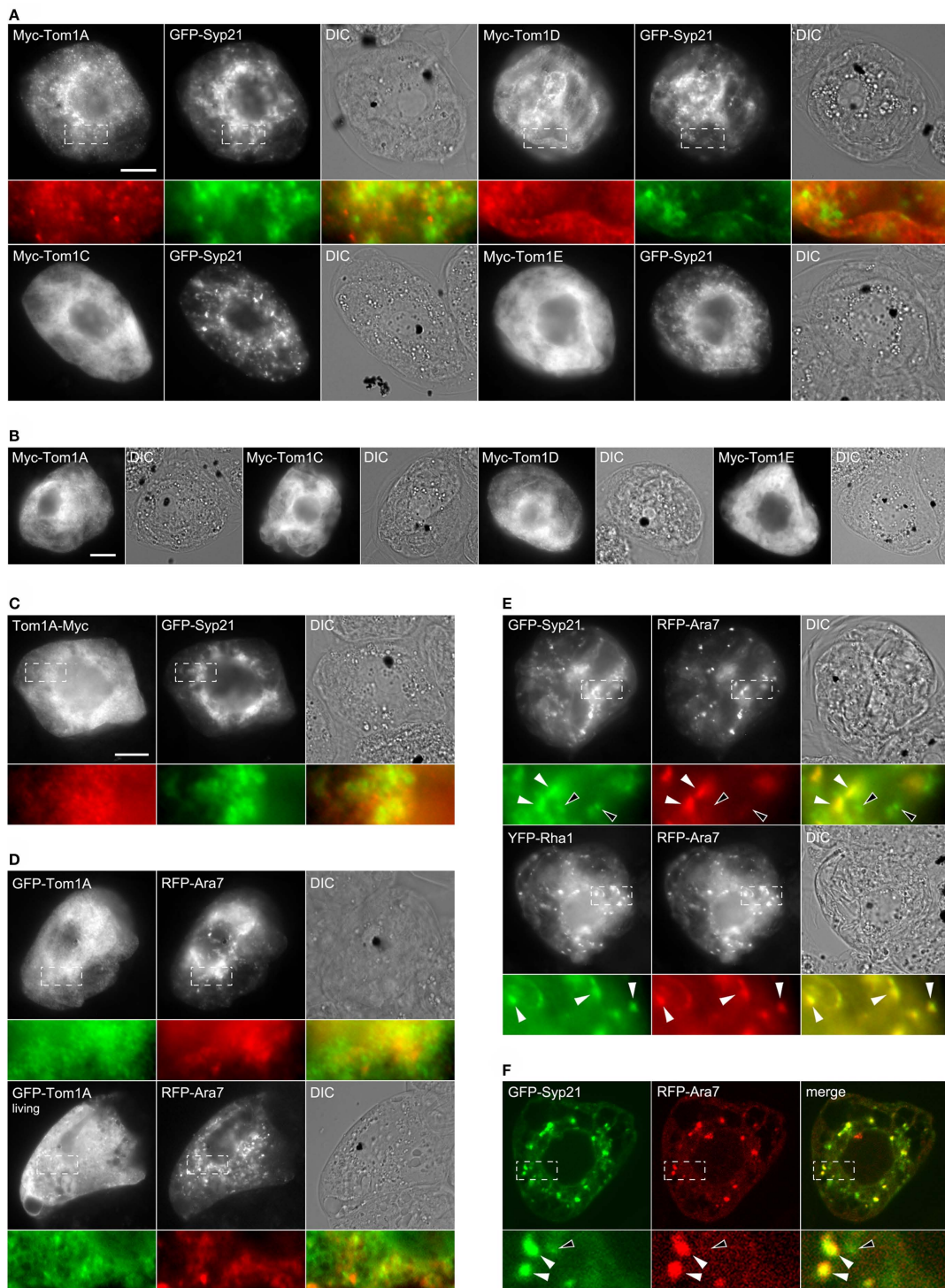
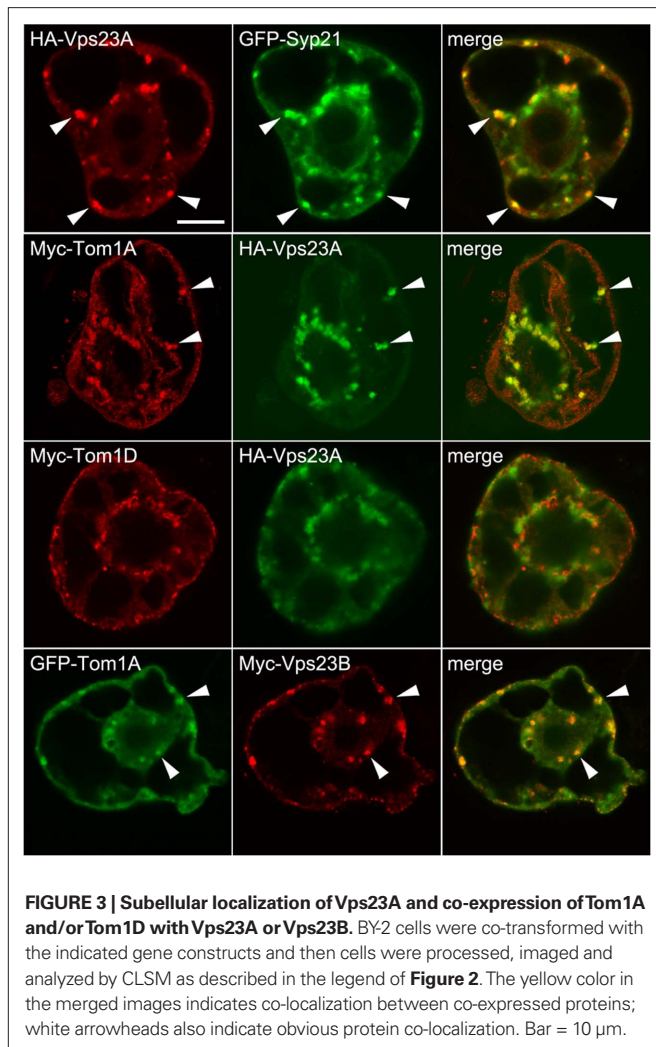


FIGURE 2 | Subcellular localization of *Arabidopsis* Tom1 proteins, GFP-Syp21, YFP-Rha1, and RFP-Ara7. BY2 cells were either transiently (co-)transformed with either **(A)** various Myc-tagged Tom1 proteins and GFP-Syp21, **(B)** the same Myc-Tom1 proteins on their own, **(C)** Tom1A-Myc and GFP-Syp21, **(D)** GFP-Tom1A and RFP-Ara7, **(E)** GFP-Syp21 and RFP-Ara7 or YFP-Rha1 and RFP-Ara7, or **(F)** GFP-Syp21 and RFP-Ara7. Cells were then either formaldehyde-fixed and processed for immuno-epifluorescence microscopy or [in **(F)**] CLSM. Alternatively, cells [in **(D)** bottom row] were viewed living (i.e., non-fixed) using epifluorescence

microscopy. Each micrograph is labeled at the top left with the name of the (co-) expressed protein construct. Also shown is the corresponding differential interference contrast (DIC) image or [in **(F)**] merged image for each set of (co-) transformed cell(s). Hatched boxes in [**(A)** and **(C-F)**] represent the portion of cells shown at higher magnification and colorized in the panels below. The yellow color in the merged images indicates co-localization between co-expressed proteins; white arrowheads [in **(E,F)**] also indicate obvious protein co-localization, while the open arrowheads in **(E,F)** indicate obvious non-co-localization. Bar = 10 μ m.



et al., 2008; Blanc et al., 2009). Additional studies of the *Arabidopsis* Tom1-related protein family, Vps23 homologs, plus the multitude of other uncharacterized ubiquitin-binding proteins encoded in the *Arabidopsis* genome that may function in MVB protein cargo selection (Leung et al., 2008) are needed in order to better understand the potential role of an “alternate” ESCRT-0 complex in plants. This task will also need to take into consideration that the Tom1 family members display distinct organ/tissue expression patterns and thus the subcellular localization of these proteins (as well as all the other ESCRT proteins examined in this study) should also be studied *in planta*. There is also a possibility that specific ubiquitinated MVB cargo proteins may serve to initiate the assembly of an ESCRT-0 complex, notably, several candidates have been recently identified as plant ESCRT cargo proteins (Spitzer et al., 2009; Viotti et al., 2010).

In addition to Vps23A and Vps23B, the putative ESCRT-I complex in *Arabidopsis* also includes Vps28A/B and Vps37A/B (**Table 1**) and while we showed via yeast two-hybrid assays (**Figure 1**) that Vps23A/B interacts with Vps28A/B and Vps37A, only Vps23A, Vps28B, and Vps37A have been shown elsewhere to form a complex in plant cells (Spitzer et al., 2006). Thus, to further investigate

the interactions detected between ESCRT-I proteins (**Figure 1**), we examined the subcellular localization of the putative Vps28A and Vps28B proteins when expressed with or without Vps23A. As shown in **Figure 4A**, both Myc-tagged Vps28A and Vps28B localized exclusively to the cytosol in BY-2 cells co-expressing GFP-Syp21, similar to the cytosolic localization of ectopically expressed Vps28 proteins in other organisms (Bishop and Woodman, 2001). By contrast, co-expression of Myc-Vps28A or Myc-Vps28B with HA-Vps23A resulted in both sets of proteins being colocalized partially to the cytosol and also to the periphery of large, ring-like structures (**Figure 4B**); shown also in **Figure 4B** (bottom row) are three related CLSM 3D projection images illustrating the localization of Myc-Vps28A in the large, ring-like structures found in an Myc-Vps28A and HA-Vps23A co-transformed cell. While similar structures were not observed in cells co-expressing any of these proteins with GFP-Syp21 alone (**Figures 3A and 4A**), these structures were readily observed in cells triple-transformed with Myc-Vps28A (or Myc-Vps28B), HA-Vps23A, and GFP-Syp21, wherein all three proteins colocalized (**Figure 4C**; results presented only for co-expressed Myc-Vps28A-HA-Vps23-GFP-Syp21), indicating they are derived from MVBs.

The relocation of Vps28 to MVB-derived structures upon co-expression with Vps23A is consistent with its classification as a core ESCRT-I component. Furthermore, the formation of these structures is reminiscent of the aberrant MVB-related structures or so-called “class E compartments” formed in yeast or mammalian cells upon over-expression or deletion of certain ESCRT components (or mutants versions thereof) that act in a dominant-negative fashion to disrupt normal ESCRT function (Roxrud et al., 2010). While we do not know the ultrastructure of the class E-like compartments in Vps23 and Vps28-co-transformed BY-2 cells (**Figure 4**) or the molecular mechanism underlying their formation, the appearance of these unique structures, combined with the observation that *Arabidopsis* Vps23 and Vps28 interact directly (**Figure 1**; Spitzer et al., 2006) provides further evidence that these proteins function together in MVB biogenesis. On the other hand, until Vps23 and Vps28 have been studied in more detail, we also urge caution in interpretation of results obtained from studies of the subcellular localization and/or MVB morphology changes associated with expression of these proteins (or any other plant ESCRT protein described in this study), and their extrapolation to cellular function(s).

As mentioned previously, in yeast and mammals, ESCRT-II is recruited to the endosomal membrane by ESCRT-I, where it plays an essential role in the concentration of ubiquitinated cargo proteins and the recruitment of ESCRT-III (reviewed in Hurley and Hanson, 2010; Peel et al., 2010). As shown in **Figure 5A**, HA-Vps36 localized in BY-2 cells to the plasma membrane and to numerous small punctae/globular or ring-like structures that occasionally colocalized with GFP-Syp21. Myc-Vps25, a second component of ESCRT-II that we showed interacts directly with Vps36 (**Figure 1**; **Figure S3** in Supplementary Material) localized exclusively to the cytosol when co-expressed with GFP-Syp21 (**Figure 5A**), but was localized primarily to the plasma membrane when co-expressed with HA-Vps36 (**Figure 5B**); refer also to CLSM images in **Figure 5B** (bottom row) confirming the co-localization of HA-Vps36 and Myc-Vps25 at the plasma membrane ($r = 0.90 \pm 0.10$). Together,

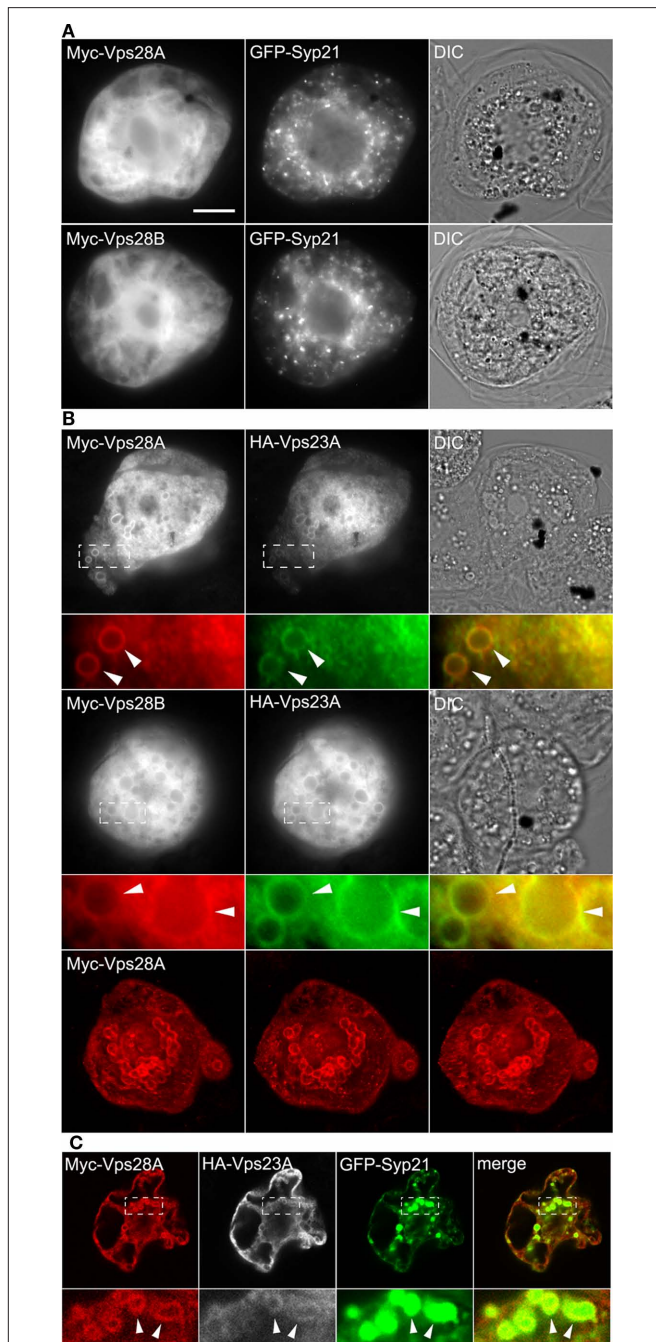


FIGURE 4 | Subcellular localization of Vps28A and Vps28B and co-expression of Vps28A or Vps28B with Vps23A. BY-2 cells were co-transformed with the indicated gene constructs and then cells were processed, imaged, and analyzed either by (A,B) epifluorescence microscopy or [(B) bottom row and (C)] CLSM as described in the legend of Figure 2. The yellow color in the corresponding merged images indicates co-localization between co-expressed proteins; white arrowheads also indicate obvious protein co-localization in the large, ring-like MVB-related structures. Note that the CLSM images presented in [(B) bottom row] are three different rotations (i.e., left -15° , center, and right $+15^\circ$) obtained from the same 3D projection (full z-series) of immunostained Myc-Vps28A in a Myc-Vps28A and HA-Vps23A co-transformed cell; refer also to Figure S4 in Supplementary Material for the corresponding movie. The CLSM images of the triple-transformed cell in (C) are single z-sections. Bar = 10 μ m.

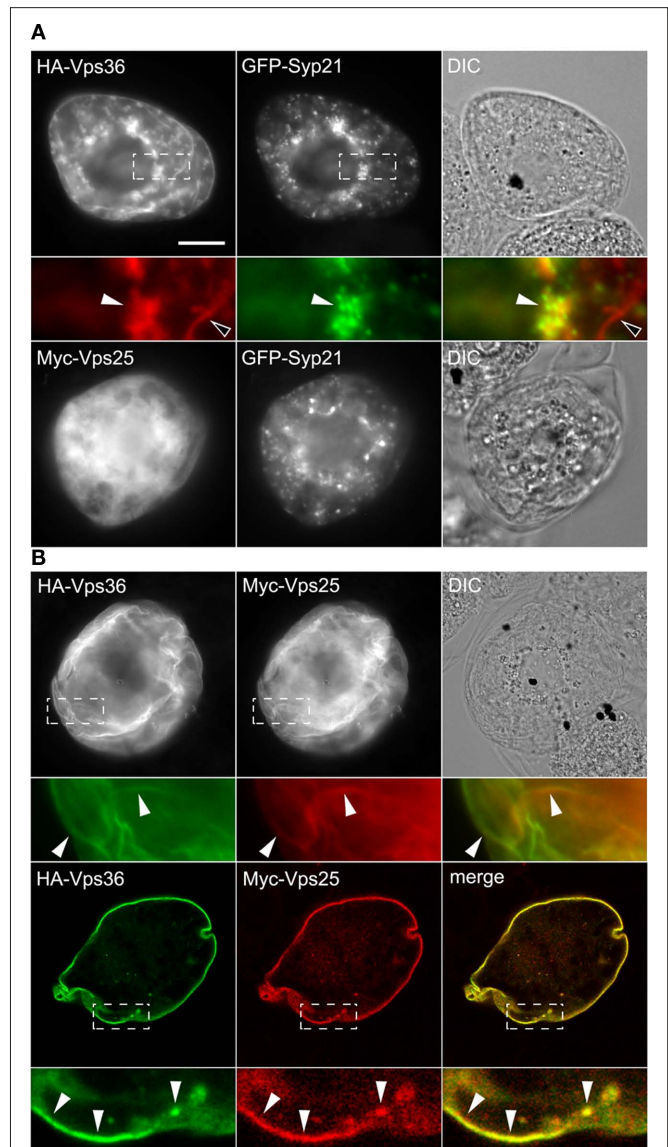


FIGURE 5 | Subcellular localization of Vps25 and Vps36. BY-2 cells were co-transformed with the indicated gene constructs and then cells were processed, imaged, and analyzed either by epifluorescence microscopy [(A,B) top row] or [(B) bottom row] CLSM as described in the legend of Figure 2. The yellow color in the corresponding merged images indicates co-localization between co-expressed proteins; white arrowheads also indicate obvious protein co-localization, while open arrowheads in (A) indicate the localization of HA-Vps36 (but not co-expressed GFP-Syp21) at the plasma membrane. Bar = 10 μ m.

these data are consistent with the premise that these two proteins function together as part of the ESCRT-II complex in *Arabidopsis*, just as they do in yeasts and mammals (Hurley and Hanson, 2010; Peel et al., 2010). However, the functional significance of the plasma membrane localization of Vps36 (and co-expressed Vps25) is still unknown and needs to be confirmed *in planta*, and further investigation of ESCRT-II and the functional relationship between Vps36 and Vps25 in *Arabidopsis* may reveal additional and/or unique roles for ESCRT-II in plants.

We examined next the subcellular localization of several putative *Arabidopsis* ESCRT-III components, including Vps20A, Vps20B, and Snf7A. Based on the working models for ESCRT in yeast and mammals (Hurley and Hanson, 2010; Peel et al., 2010), each of the four core components of ESCRT-III (e.g., yeast Vps2, Vps20, Vps24, and Snf7; **Table 1**) contain a similar domain organization, including an N-terminal basic domain required for membrane interaction and (homo- and/or hetero-) oligomerization, and a C-terminal acidic autoinhibitory domain that prevents their oligomerization and recruitment from the cytosol to endosomes. By a mechanism that is not fully understood, autoinhibition is relieved, allowing the ESCRT-III proteins to be sequentially assembled on the endosomal membrane as two subcomplexes; the Vps20-Snf7 subcomplex that binds to the endosomal membrane through the N-terminal myristoylation of Vps20 and a direct interaction with Vps25 of ESCRT-II, and

the Vps2-Vps24 subcomplex that binds via an interaction between Vps24 and Snf7A. Consistent with this model, our yeast two-hybrid assays (**Figure 1**) revealed that both of the putative *Arabidopsis* Vps20 isoforms (Vps20A and Vps20B) interact with Vps25, as well as with Snf7A and Snf7B. Moreover, both Snf7A/B and all of the other putative *Arabidopsis* ESCRT-III proteins share a relatively high degree of primary sequence and secondary structure similarity with their yeast and mammalian counterparts (Winter and Hauser, 2006; Leung et al., 2008), including conserved N-terminal basic and C-terminal acidic regions. In addition, both *Arabidopsis* Vps20A/B, like Vps20 proteins in other organisms, possess a predicted N-terminal myristoylation signal (Leung et al., 2008).

As shown in **Figure 6A**, both Vps20A-Myc and Vps20B-Myc, consisting of full-length *Arabidopsis* Vps20A and Vps20B appended to the Myc-epitope tag at their C terminus in order to preserve their

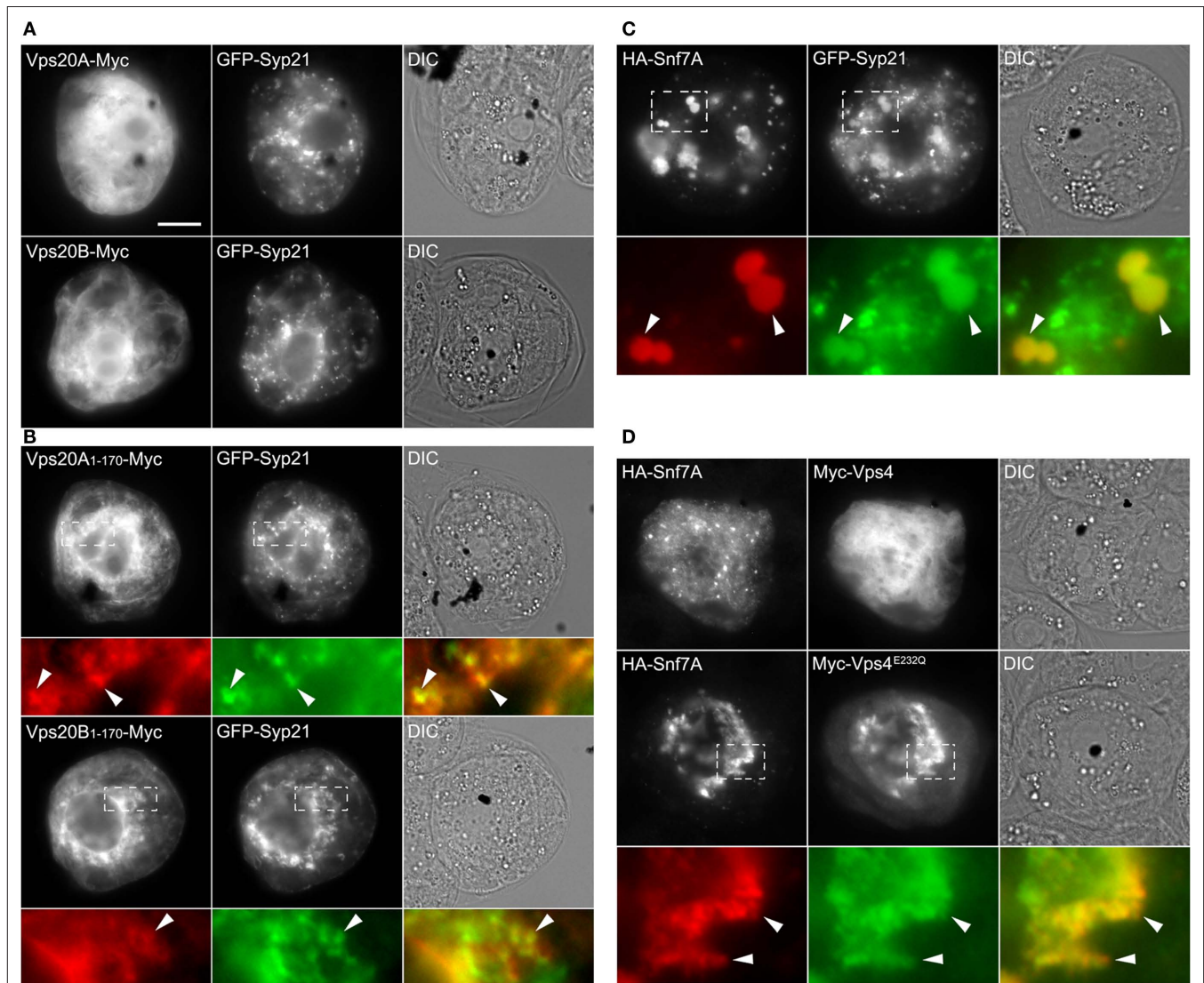


FIGURE 6 | Subcellular localization of full-length and C-terminal-truncated versions of Vps20A and Vps20B, and co-expression of Snf7A and Vps4 or Vps4^{E232Q}. (A–D) BY-2 cells were co-transformed with the indicated gene constructs and then cells were processed, imaged and analyzed by

epifluorescence microscopy as described in the legend of **Figure 2**. The yellow color in the corresponding merged images [in (B–D)] indicates co-localization, between co-expressed proteins; white arrowheads indicate obvious protein co-localization including in the enlarged globular-like structures in (C). Bar = 10 μ m.

putative N-terminal myristoylation signal, localized exclusively to the cytosol in BY-2 cells. By contrast, C-terminal-mutant versions of both proteins, namely Vps20A₁₋₁₇₀-Myc and Vps20B₁₋₁₇₀-Myc (consisting of their N-terminal 1–170 out of ~220 amino acid residues), localized to the cytosol and to punctate/globular structures, at least some of which also contained co-expressed GFP-Syp21 (**Figure 6B**). Combined, these results are similar to those for the localization of human (full-length) Chmp6 (the mammalian homolog of *Arabidopsis* Vps20) in the cytosol and the partial localization of a C-terminally truncated mutant version of Chmp6 to endosomes (Peck et al., 2004), suggesting that a C-terminal auto-inhibitory mechanism may be conserved between Chmp6 and *Arabidopsis* Vps20.

As shown in **Figure 6C**, the putative *Arabidopsis* Snf7A (i.e., HA-Snf7A) localized in BY-2 cells to punctae and large, globular-like structures that mostly colocalized with co-expressed GFP-Syp21. Given the ability of Snf7 and Chmp4 yeast and mammalian cells, respectively, to form large, higher-ordered polymers on the endosomal surface (Teis et al., 2010) and induce the formation of aberrant MVB-related structures upon their over-expression in cells (Peck et al., 2004; Boysen and Mitchell, 2006), it is possible that the large globular structures observed in BY-2 cells may be also the result of the assembly of abnormal Snf7A oligomers. This premise is supported, albeit indirectly, by the ability of *Arabidopsis* Snf7A/B to interact in yeast two-hybrid assays (**Figure 1**), just as their yeast and mammalian counterparts do (Nikko and André, 2007).

Following membrane scission, ESCRT-III subunits (mainly Snf7) are disassembled and recycled to the cytosol for further rounds of vesicle formation, a process that is mediated by Vps4 and its regulators in yeasts and mammals (Hurley and Hanson, 2010; Peel et al., 2010), and, based on available data, also in plants (Jou et al., 2006; Haas et al., 2007; Shahriari et al., 2010). Unexpectedly, however, Vps4 and Snf7A/B did not interact in the yeast two-hybrid assay (**Figure 1**), which contrasts the interaction data reported elsewhere (Shahriari et al., 2010), and Myc-Vps4 was localized exclusively to the cytosol in BY-2 cells co-expressing HA-Snf7A (**Figure 6D**). We therefore took advantage of a catalytically inactive version of Vps4 that is well-known in yeasts and mammals to have a potent dominant-negative effect on MVB biogenesis by binding irreversibly to MVBs and “trapping” the ESCRT(-III) machinery on the MVB surface (Babst et al., 1998). The equivalent mutation in the *Arabidopsis* protein (Vps4^{E232Q}) has also been shown to be catalytically inactive and disrupt MVB biogenesis in plant cells (Haas et al., 2007; Shahriari et al., 2010). As shown also in **Figure 6D**, when HA-Snf7A was co-expressed with Myc-Vps4^{E232Q}, both proteins mostly colocalized in irregular-shaped structures that appeared to be distinct from punctate and large, globular-like structures observed in cells expressing HA-Snf7A and GFP-Syp21, further supporting the classification of Snf7A (and Snf7B) as a component of ESCRT-III, and suggesting a possible functional relationship between Snf7A and Vps4, just as in other organisms (Hurley and Hanson, 2010; Peel et al., 2010).

CONCLUSION

In recent years, there has been a proliferation in studies of the ESCRT machinery in yeasts and mammals, wherein ESCRT has been shown to participate in a remarkable range of cellular processes (Carlton

and Martin-Serrano, 2009; Hurley and Hanson, 2010; Peel et al., 2010; Roxrud et al., 2010). However, while homologs of most of the ESCRT proteins exist in plants (**Table 1**), only relatively few of these have been characterized in detail and, thus, the main objective of this study was to gain a better, more global understanding of the *Arabidopsis* ESCRT machinery. Toward that end, we surveyed many of the known and putative ESCRT components in *Arabidopsis* in terms of their protein–protein interaction network and subcellular localizations. In doing so, we were able to not only integrate the results of these experiments with those obtained from other studies on some of the same *Arabidopsis* ESCRT proteins, but also to directly compare and contrast features of the plant ESCRT machinery with those reported for ESCRT in other evolutionarily diverse organisms. This latter point is perhaps best exemplified by our systematic analysis of the *Arabidopsis* ESCRT interactome using the yeast two-hybrid assay (**Figure 1**), since a similar strategy was employed for initially characterizing interactions among ESCRT proteins in yeasts and humans (Martin-Serrano et al., 2003; von Schwedler et al., 2003), and, just like it has done so for these organisms, our yeast two-hybrid results should now serve as a framework for generating testable working models for ESCRT function(s) in plants.

In examining the subcellular localization of several putative or known ESCRT proteins, we also observed the formation of aberrant MVB-related structures when some of these proteins were expressed or co-expressed in plant (BY-2) cells [e.g., Vps23A and Vps28A (**Figure 4B**), Snf7A (**Figure 6C**), or Snf7A and Vps4^{E232Q} (**Figure 6D**)]. Notably, similar abnormal MVB structures are formed upon (co)expression of their mammalian and/or yeast counterparts (or mutant versions thereof; reviewed in Roxrud et al., 2010), implying that not only do these plant ESCRT proteins operate mechanistically in a similar manner, but that the subsequent characterization of these abnormal MVB-related structures in plant cells will be informative in understanding normal ESCRT function, just as they have been for understanding ESCRT in yeasts and mammals. Of course, the fact that many of the known and putative plant ESCRT proteins exist as paralogs (Mullen et al., 2006; Spitzer et al., 2006; Winter and Hauser, 2006; Leung et al., 2008) and are differentially expressed in various organs/tissues (i.e., based on publicly available microarray databases) adds layers of complexity to the examination and determination of their biological roles *in planta*, complexity that must be also reconciled with the highly conserved nature of ESCRT interactions and operation. Moreover, any complete understanding of ESCRT in plants will undoubtedly be challenged by our need to know more about the distinct and highly dynamic nature of the plant endosomal pathway overall, such as the *trans*-Golgi network acting as an early endosome in MVB formation and the functional diversification of MVBs (Foresti et al., 2010; Viotti et al., 2010). Nevertheless, the data provided here combined with those from recent proteomic (Groen et al., 2008) and microscopy studies (Kang et al., 2011; Viotti et al., 2010), as well as high-throughput chemical screens (Hicks and Raikhel, 2010), should begin to shed light on these and other aspects of plant MVB biogenesis.

AUTHOR CONTRIBUTIONS

L. Richardson, A. McCartney, and R. Mullen designed the study; L. Richardson, A. Howard, N. Khuu, A. McCartney, and B. Morphy performed the yeast two-hybrid assays and/or

co-immunoprecipitations; L. Richardson and S. Gidda carried out the subcellular localization studies; L. Richardson, A. Howard, S. Gidda, and A. McCartney generated the gene constructs; and L. Richardson and R. Mullen wrote the paper.

ACKNOWLEDGMENTS

We thank Drs T. Ueda, M. Sato, E. Nielsen, and M. Otegui for their generous gifts of plasmids used in this study. We are also indebted to members of our laboratory for their helpful discussions during the course of this work and their comments during the preparation of the manuscript. This work was supported by a grant from the Natural Sciences and Engineering Research Council of Canada (NSERC) to R. Mullen, as well as partial financial support for S. Gidda provided by a grant from the Ontario Research and Development Challenge Fund (Ontario Centre for Agricultural Genomics) to S. Rothstein. R. Mullen holds a University of Guelph Research Chair and L. Richardson is a recipient of an NSERC CGS-D Postgraduate Scholarship.

NOTE ADDED IN PROOF

During review of this manuscript, Shahriari and workers (Plant Mol. Biol. 2011, 76:85–96) also analyzed the *Arabidopsis* protein-protein interaction network using the yeast two-hybrid assay, as well as biomolecular fluorescence complementation.

SUPPLEMENTARY MATERIAL

The Movie 1 for this article can be found online at http://www.frontiersin.org/plant_cell_biology/10.3389/fpls.2011.00020/abstract

FIGURE S1 | Protein immunoblot analysis of yeast expressing individual

AD- or BD-*Arabidopsis* ESCRT fusion proteins. Yeast were transformed individually with plasmids encoding either (A) GAL4-AD or (B) GAL4-BD ESCRT fusion proteins or the corresponding “empty” AD or BD control plasmids, were cultured in non-selective media and then processed for SDS-PAGE and immunoblotting (see Materials and Methods for details). Shown are representative immunoblots probed with either (A) α -Myc antibodies, which recognize the Myc-epitope tag located between the GAL4-AD moiety and ESCRT

protein, or (B) α -HA antibodies, which recognize the HA epitope tag located between the GAL4-BD moiety and ESCRT protein. All of the immunodetected AD/BD-ESCRT fusion proteins (indicated with upward or downward arrows) were consistent with their expected (ca.) sizes; although, in some cases, smaller, additional bands were also observed, likely truncated version of these proteins due to internal translation initiation and/or partial protein degradation. Note also in (A) a non-specific, ~80 kDa endogenous yeast polypeptide (marked with an asterisk) was immunodetected in protein blots probed with α -Myc antibodies. Numerical values to the left of blots are the molecular masses (in kDa) of protein standards.

FIGURE S2 | Representative two-hybrid-assay plates showing the relative growth of selected AD- and BD-*Arabidopsis* ESCRT co-transformed yeast strains.

Yeast harboring (co-transformed) either individual pairs of each of the positive two-hybrid-interacting AD- and BD-ESCRT fusion proteins (refer to shaded boxes in Figure 2) or the corresponding “empty” AD or BD control plasmids (refer to the top two rows in Figure 2), were (replica) spotted onto agar plates containing either (B) low-stringency selection media (SD-LT), (C) high-stringency selection media (SD-LTHA) without 3-AT, or (D) SD-LTHA with 3-AT, and incubated for 5 days at 30°C. Shown in (A) are the locations (drawn as circles) on the plates of each of the co-transformed yeast strains examined, as well as the specific combinations of AD- and BD-ESCRT (or “empty vector”) plasmids they harbor (numbered 1–150).

FIGURE S3 | Co-immunoprecipitations of *Arabidopsis* ESCRT proteins *in vitro*.

Plasmids encoding selected AD- or BD-ESCRT fusion proteins (which included an HA or Myc-epitope tag between the GAL4-AD or BD moieties, respectively, and the ESCRT protein) were transcribed and translated *in vitro* (see Materials and Methods for details). Translation products for specific protein pairs (referred to as “prey” and “bait”) or only the “prey” proteins serving as negative controls were mixed and incubated [as indicated below each blot (IP)] with either α -Myc or α -HA antibodies, followed by an incubation with Protein A-Sepharose and then centrifugation. Next, equivalent amounts of all co-immunoprecipitated protein fractions, as well as an aliquot of *in vitro*-synthesized “prey” protein alone (refer to the first lane in each blot) were subjected to SDS-PAGE and Western blotting with (as indicated to the left of each blot) either α -HA or α -Myc antibodies and the appropriate enzyme-linked secondary antibodies. Arrowheads at the right side of the blots indicate the migration positions of the specific immunodetected “prey” proteins. The additional lower molecular mass proteins observed in most blots are IgGs carried over from the co-immunoprecipitation reactions. Shown also (on the right) are compilations of blots of the individual HA- or Myc-tagged “bait” proteins used as input for corresponding co-immunoprecipitations reactions.

FIGURE S4 | Subcellular localization of Vps28A. Movie depicting the CLSM 3D projection (full z-series) of immunostained Myc-Vps28A in the Myc-Vps28A and HA-Vps23A co-transformed cell shown in Figure 4B (bottom row).

REFERENCES

- Babst, M., Wendland, B., Estepa, E. J., and Emr, S. D. (1998). The Vps4p AAA ATPase regulates membrane association of a Vps protein complex required for normal endosome function. *EMBO J.* 17, 2982–2993.
- Bishop, N., and Woodman, P. (2001). TSG101/mammalian Vps23 and mammalian Vps28 interact directly and are recruited to Vps4-induced endosomes. *J. Biol. Chem.* 276, 11735–11742.
- Blanc, C., Charette, S. J., Mattei, S., Aubry, L., Smith, E. W., Cosson, P., and Letourneur, F. (2009). Dictyostelium Tom1 participates to an ancestral ESCRT-0 complex. *Traffic* 10, 161–171.
- Boysen, J. H., and Mitchell, A. P. (2006). Control of Bro1-domain protein Rim20 localization by external pH, ESCRT machinery, and the *Saccharomyces cerevisiae* Rim101 pathway. *Mol. Biol. Cell* 17, 1344–1353.
- Brandizzi, F., Irons, S., Kearns, A., and Hawes, C. (2003). BY-2 cells: culture and transformation for live cell imaging. *Curr. Protoc. Cell Biol.* 1, 7.1–7.16.
- Carlton, J. G., and Martin-Serrano, J. (2009). The ESCRT machinery: new functions in viral and cellular biology. *Biochem. Soc. Trans.* 37, 195–199.
- Clark, S. M., Rosa, D. L., Dhanoa, P. K., Van Cauwenbergh, O. R., Mullen, R. T., and Shelp, B. J. (2009). Biochemical characterization, mitochondrial localization, expression, and potential functions for an *Arabidopsis* γ -aminobutyrate transaminase that utilizes both pyruvate and glyoxylate. *J. Exp. Bot.* 60, 1743–1757.
- Foresti, O., daSilva, L. L. P., and Denecke, J. (2006). Overexpression of the *Arabidopsis* syntaxin PEP12/SYP21 inhibits transport from the prevacuolar compartment to the lytic vacuole *in vivo*. *Plant Cell* 18, 2275–2293.
- Foresti, O., Gershlick, D. C., Bottanelli, F., Hummel, E., Hawes, C., and Denecke, J. (2010). A recycling-defective vacuolar sorting receptor reveals an intermediate compartment situated between prevacuoles and vacuoles in tobacco. *Plant Cell* 22, 3992–4008.
- Gidda, S. K., Shockey, J. M., Falcone, M., Kim, P. K., Rothstein, S. J., Andrews, D. W., Dyer, J. M., and Mullen, R. T. (2011). Hydrophobic-domain-dependent protein-protein interactions mediate the localization of GPAT enzymes to ER subdomains. *Traffic* 12, 452–472.
- Groen, A. J., de Vries, S. C., and Lilley, K. S. (2008). A proteomics approach to membrane trafficking. *Plant Physiol.* 147, 1584–1589.
- Gruenberg, J., and Stenmark, H. (2004). The biogenesis of multivesicular endosomes. *Nat. Rev. Mol. Cell Biol.* 5, 317–323.
- Haas, T. J., Sliwinski, M. K., Martínez, D. E., Preuss, M., Ebine, K., Ueda, T., Nielsen, E., Odorizzi, G., and Otegui, M. S. (2007). The *Arabidopsis* AAA ATPase SKD1 is involved in multivesicular endosome function and interacts with its positive regulator LYST-interacting protein 5. *Plant Cell* 19, 1295–1312.
- Hicks, G. R., and Raikhel, N. V. (2010). Advances in dissecting endomembrane trafficking with small molecules. *Curr. Opin. Plant Biol.* 13, 706–713.
- Hurley, J. H., and Hanson, P. I. (2010). Membrane budding and scission by the ESCRT machinery: it's all in the neck. *Nat. Rev. Mol. Cell Biol.* 11, 556–566.
- Jou, Y., Chiang, C.-P., Jauh, G.-Y., and Yen, H. E. (2006). Functional characterization of ice plant SKD1, an AAA-Type ATPase associated with the endoplasmic reticulum-Golgi network, and its role in adaptation to salt stress. *Plant Physiol.* 141, 135–146.
- Kang, B. H., Nielsen, E., Preuss, M. L., Mastrorarde, D., and Staehelin, L. A. (2011). Electron tomography of RabA4b- and PI-4Kb1-labeled trans

- Golgi network compartments in *Arabidopsis*. *Traffic* 12m, 313–329.
- Kato, N., Fujikawa, Y., Fuselier, T., Adamou-Dodo, R., Nishitani, A., and Sato, M. H. (2010). Luminescence detection of SNARE-SNARE interaction in *Arabidopsis* protoplasts. *Plant Mol. Biol.* 72, 433–444.
- Lee, G.-J., Sohn, E. J., Lee, M. H., and Hwang, I. (2004). The *Arabidopsis* Rab5 homologues Rha1 and Ara7 localize to the prevacuolar compartment. *Plant Cell Physiol.* 45, 1211–1220.
- Leung, K. F., Dacks, J. B., and Field, M. C. (2008). Evolution of the multivesicular body ESCRT machinery: retention across the eukaryotic lineage. *Traffic* 9, 1698–1716.
- Lingard, M. J., Gidda, S. K., Bingham, S., Rothstein, S. J., Mullen, R. T., and Trelease, R. N. (2008). *Arabidopsis* peroxin11c-e, fission1b, and dynamin-related protein3A cooperate in cell cycle-associated replication of peroxisomes. *Plant Cell* 20, 1567–1585.
- Martin-Serrano, J., Yaravoy, A., Perez-Caballero, D., and Bieniasz, P. D. (2003). Divergent retroviral late-budding domains recruit vacuolar protein sorting factors by using alternative adaptor proteins. *Proc. Natl. Acad. Sci. U.S.A.* 100, 12414–12419.
- Miao, Y. S., and Jiang, L. W. (2007). Transient expression of fluorescent fusion proteins in protoplasts of suspension cultured cells. *Nature Protoc.* 2, 2348–2353.
- Miller, J. B. (1972). "Assay for β -galactosidase," in *Experiments in Molecular Genetics*, ed. J. H. Miller (Cold Spring Harbor: Cold Spring Harbor Laboratory), 352–355.
- Mo, B., Tse, Y. C., and Jiang, L. (2006). Plant prevacuolar/endosomal compartments. *Int. Rev. Cytol.* 253, 95–129.
- Mullen, R. T., McCartney, A. W., Flynn, C. R., and Smith, G. S. T. (2006). Peroxisome biogenesis and the formation of multivesicular peroxisomes during tombusvirus infection: a role for ESCRT? *Can. J. Bot.* 84, 551–564.
- Müller, J., Metzbach, U., Menzel, D., and Samaj, J. (2007). Molecular dissection of endosomal compartments in plants. *Plant Physiol.* 145, 293–304.
- Nikko, E., and André, B. (2007). Split-ubiquitin two-hybrid assay to analyze protein-protein interactions at the endosome: application to *Saccharomyces cerevisiae* Bro1 interacting with ESCRT complexes, the Doa4 ubiquitin hydrolase, and the Rsp5 ubiquitin ligase. *Eukaryot. Cell* 6, 1266–1277.
- O'Quin, J. B., Mullen, R. T., and Dyer, J. M. (2009). Addition of an N-terminal epitope tag significantly increases the activity of plant fatty acid desaturases expressed in yeast cells. *Appl. Microbiol. Biotechnol.* 83, 117–125.
- Otegui, M. S., and Spitzer, C. (2008). Endosomal functions in plants. *Traffic* 9, 1589–1598.
- Peck, J. W., Bowden, E. T., and Burbelo, P. D. (2004). Structure and function of human Vps20 and Snf7 proteins. *Biochem. J.* 377, 693–700.
- Peel, S., Macheboeuf, P., Martinelli, N., and Weissenhorn, W. (2010). Divergent pathways lead to ESCRT-III-catalyzed membrane fission. *Trends Biochem. Sci.* 36, 199–210.
- Raymond, C. K., Howald-Stevenson, I., Vater, C. A., and Stevens, T. H. (1992). Morphological classification of the yeast vacuolar protein sorting mutants: evidence for a prevacuolar compartment in class E vps mutants. *Mol. Biol. Cell* 3, 1389–1402.
- Robinson, D. G., Jiang, L., and Schumacher, K. (2008). The endosomal system of plants: charting new and familiar territories. *Plant Physiol.* 147, 1482–1492.
- Roxrud, I., Stenmark, H., and Malerød, L. (2010). ESCRT & Co. *Biol. Cell* 102, 293–318.
- Schellmann, S., and Pimpl, P. (2009). Coats of endosomal protein sorting: retromer and ESCRT. *Curr. Opin. Plant Biol.* 12, 670–676.
- Shahriari, M., Keshavaiah, C., Scheuring, D., Sabovljevic, A., Pimpl, P., Häusler, R. E., Hülskamp, M., and Schellmann, S. (2010). The AAA-type ATPase AtSKD1 contributes to vacuolar maintenance of *Arabidopsis thaliana*. *Plant J.* 64, 71–85.
- Shen, B., Li, C., Min, Z., Meeley, R. B., Tarczyński, M. C., and Olsen, O.-A. (2003). Sal1 determines the number of aleurone cell layers in maize endosperm and encodes a class E vacuolar sorting protein. *Proc. Natl. Acad. Sci. U.S.A.* 100, 6552–6557.
- Shestakova, A., Hanono, A., Drosner, S., Curtiss, M., Davies, B. A., Katzmann, D. J., and Babst, M. (2010). Assembly of the AAA ATPase Vps4 on ESCRT-III. *Mol. Biol. Cell* 21, 1059–1071.
- Shirakawa, M., Ueda, H., Shimada, T., Koumoto, Y., Shimada, T. L., Kondo, M., Takahashi, T., Okuyama, Y., Nishimura, M., and Hara-Nishimura, I. (2010). *Arabidopsis* Qa-SNARE SYP2 proteins localized to different subcellular regions function redundantly in vacuolar protein sorting and plant development. *Plant J.* 64, 924–935.
- Shockey, J. M., Gidda, S. K., Chapital, D. C., Kuan, J. C., Dhanoa, P. K., Bland, J. M., Rothstein, S. J., Mullen, R. T., and Dyer, J. M. (2006). Tung tree DGAT1 and DGAT2 have nonredundant functions in triacylglycerol biosynthesis and are localized to different subdomains of the endoplasmic reticulum. *Plant Cell* 18, 2294–2313.
- Spitzer, C., Reyes, F. C., Buono, R., Sliwinski, M. K., Haas, T. J., and Otegui, M. (2009). The ESCRT-related CHMP1A and B proteins mediate multivesicular body sorting of auxin carriers in *Arabidopsis* and are required for plant development. *Plant Cell* 21, 749–766.
- Spitzer, C., Schellmann, S., Sabovljevic, A., Shahriari, M., Keshavaiah, C., Bechtold, N., Herzog, M., Müller, S., Hanisch, F.-G., and Hülskamp, M. (2006). The *Arabidopsis* elch mutant reveals functions of an ESCRT component in cytokinesis. *Development* 133, 4679–4689.
- Teis, D., Saksena, S., Judson, B. L., and Emr, S. D. (2010). ESCRT-II coordinates the assembly of ESCRT-III filaments for cargo sorting and multivesicular body vesicle formation. *EMBO J.* 29, 871–883.
- Tian, Q., Olsen, L., Sun, B., Lid, S. E., Brown, R. C., Lemmon, B. E., Fosnes, K., Gruis, D., Opsahl-Sorteberg, H.-G., Otegui, M. S., and Olsen, O.-A. (2007). Subcellular localization and functional domain studies of defective kernel1 in maize and *Arabidopsis* suggest a model for aleurone cell fate specification involving CRINKLY4 and supernumerary aleurone layer1. *Plant Cell* 19, 3127–3145.
- Ueda, T., Uemura, T., Sato, M. H., and Nakano, A. (2004). Functional differentiation of endosomes in *Arabidopsis* cells. *Plant J.* 40, 783–789.
- Ueda, T., Yamaguchi, M., Uchimiya, H., and Nakano, A. (2001). Ara6, a plant-unique novel type Rab GTPase, functions in the endocytic pathway of *Arabidopsis thaliana*. *EMBO J.* 20, 4730–4741.
- Uemura, T., Morita, M. T., Ebine, K., Okatani, Y., Yano, D., Saito, C., Ueda, T., and Nakano, A. (2010). Vacuolar/prevacuolar compartment Qa-SNAREs VAM3/SYP22 and PEP12/SYP21 have interchangeable functions in *Arabidopsis*. *Plant J.* 64, 864–873.
- Uemura, T., Ueda, T., Ohniwa, R. L., Nakano, A., Takeyasu, K., and Sato, M. H. (2004). Systematic analysis of SNARE molecules in *Arabidopsis*: dissection of the post-Golgi network in plant cells. *Cell Struct. Funct.* 29, 49–65.
- Viotti, C., Bubeck, J., Stierhof, Y. D., Krebs, M., Langhans, M., van den Berg, W., van Dongen, W., Richter, S., Geldner, N., Takano, J., Jürgens, G., de Vries, S. C., Robinson, D. G., and Schumacher, K. (2010). Endocytic and secretory traffic in *Arabidopsis* merge in the trans-Golgi network/early endosome, an independent and highly dynamic organelle. *Plant Cell* 22, 1344–1357.
- von Schwedler, U. K., Stuchell, M., Müller, B., Ward, D. M., Chung, H.-Y., Morita, E., Wang, H. E., Davis, T., He, G.-P., Cimbora, D. M., Scott, A., Kräusslich, H.-G., Kaplan, J., Morham, S. G., and Sundquist, W. I. (2003). The protein network of HIV budding. *Cell* 114, 701–713.
- Wang, T., Liu, N. S., Seet, L.-F., and Hong, W. (2010). The emerging role of VHS domain-containing Tom1, Tom1L1 and Tom1L2 in membrane trafficking. *Traffic* 11, 1119–1128.
- Winter, V., and Hauser, M. T. (2006). Exploring the ESCRTing machinery in eukaryotes. *Trends Plant Sci.* 11, 115–123.
- Yanagida-Ishizaki, Y., Takei, T., Ishizaki, R., Imakagura, H., Takahashi, S., Shin, H. W., Katoh, Y., and Nakayama, K. (2008). Recruitment of Tom1L1/Scra8 to endosomes and the mid-body by Tsg101. *Cell Struct. Funct.* 33, 91–100.
- Yang, K. S., Jin, U. H., Kim, J., Song, K., Kim, S. J., Hwang, I., Lim, Y. P., and Pai, H. S. (2004). Molecular characterization of NbCHMP1 encoding a homolog of human CHMP1 in *Nicotiana benthamiana*. *Mol. Cells* 17, 255–261.

Conflict of Interest Statement: The authors declare that the research was conducted in the absence of any commercial or financial relationships that could be construed as a potential conflict of interest.

Received: 15 March 2011; accepted: 03 June 2011; published online: 22 June 2011.

Citation: Richardson LGL, Howard ASM, Khuu N, Gidda SK, McCartney A, Morphy BJ and Mullen RT (2011) Protein-protein interaction network and subcellular localization of the *Arabidopsis thaliana* ESCRT machinery. *Front. Plant Sci.* 2:20. doi: 10.3389/fpls.2011.00020

This article was submitted to *Frontiers in Plant Cell Biology*, a specialty of *Frontiers in Plant Science*.

Copyright © 2011 Richardson, Howard, Khuu, Gidda, McCartney, Morphy and Mullen. This is an open-access article subject to a non-exclusive license between the authors and Frontiers Media SA, which permits use, distribution and reproduction in other forums, provided the original authors and source are credited and other Frontiers conditions are complied with.